Chemical Engineering Journal 102 (2004) 71–82

Chemical Engineering Journal

www.elsevier.com/locate/cej

Dynamic analysis of mass transfer at vertically oscillating surfaces

H. Gomaa*, A.M. Al Taweel

Chemical Engineering Department, Dalhousie University, P.O. Box 1000, Halifax, NS, Canada B3J 2X4

Received 9 September 2003; accepted 22 February 2004

Abstract

The dynamical behavior of mass transfer at vertically oscillating surfaces is investigated both experimentally and analytically. The presence of small oscillatory component superimposed on a large steady one that does not reach zero during reversal times was explained in terms of the interaction between a "quasi-steady oscillatory" mechanism near the leading edge of the active mass transfer area, and a "steady diffusive" one far from it. A model was developed that predicted both the time average mass transfer rates, and the time dependent oscillatory component with accuracy being highest at large L/a ratios. Based on the analysis, the model can be used for describing mass transfer at vertically oscillating flat surfaces, and for modeling of systems where knowledge of the mass transfer dynamical behavior is of interest. For cases where only the time average mass transfer rate is required, the contribution of the oscillatory motion to the mass transfer enhancement at vertical surfaces can be estimated adequately using mixed "forced-natural" convections correlation, with the forced convection component estimated based on the time average vibrational Reynolds number of the vibrating surface $Re_v = a\omega L/v$.

Keywords: Mass transfer; Vibration; Enhancement; Process intensification

1. Introduction

The use of oscillatory motion has been known as an effective method for enhancing the performance of processes limited by concentration polarization and surface fouling, such as membrane filtration and electrochemical reactions. It received increasing attention recently with the emergence of applications requiring higher transfer rates and specificity in mixing that could not be achieved by conventional mixing or increasing flow rates [1]. Application of oscillatory motion can be achieved by either pulsating the liquid [2,3], or vibrating the surface [4,5]. Although both methods have the same objective of creating an oscillatory velocity vector between the solid surface and the fluid medium, the former is less energy efficient since it accelerates and de-accelerates significant portion of the fluid as compared to oscillating the solid surface [6].

Among the many examples where oscillatory motion have resulted in significant performance improvement are those involving membrane separation such as ultrafiltration, microfiltration, electrodialysis, and electrophoresis, where three to six-folds increase in transfer rates was reported [7–10]. It has also been beneficial in medical engineering applications such as enhancing mass transfer rate in blood oxygenator by a factor of three [11], and increasing plasma filtration rate by a factor of five in donor plasmapheresis membrane separator [12]. In the field of biochemical engineering oscillatory motion has been reported to enhance mass transfer rate in biofilm and membrane bioreactor by more than five-folds [13,14], and to overcome the challenges in mammalian cell bioreactors operation created by the detrimental impact of the impeller shear on cells viability in a mechanically agitated contactors [15].

Application of oscillatory motion in electrochemical processing has been of particular interest due to its ability to enhance mass transfer rate, current density and system energy utilization. Recently, it was shown that more than 20–fold increase in the mass transfer rate could be achieved by vibrating vertical electrodes along their length [4]. Among its applications in that field are electrochemical processing, electroplating, metal recovery from bio-leaching solutions, and more recently manufacture of Printed Wiring Board where electroplating is re-emerging of as the preferred technology for producing "sub-micron multi-level metallization" in ultra large scale integration [16–22].

Although the influence of oscillatory motion on transfer enhancement has been demonstrated, the question of understanding its mechanisms and their contribution to the enhancement factor still poses an issue of fundamental importance from the standpoint of both basic research, and the

* Corresponding author. Present address: P.O. Box 2103, Port Elgin, Ont., Canada N0H 2C0. Fax: +1-519-797-1956.
E-mail address: gomaah@bmts.com (H. Gomaa).

1385-8947/$ – see front matter © 2004 Elsevier B.V. All rights reserved.
doi:10.1016/j.cej.2004.02.004

Nomenclature

a	amplitude of plate vibration (mm)
A	plate active surface area (mm^2)
c	concentration of the ferri-ferrocyanide (mol/mm^3)
D	diffusion coefficient (mm^2/s)
f	frequency of electrode Vibration (Hz)
F	faraday's constant (C/Equiv.)
g	acceleration of gravity (cm/s^2)
Gr	Grashof number, $Gr = \alpha\,\Delta c g L^3/\nu^2$
h	dimensionless function, Eq. (10)
I_L	limiting current (C/s)
L	length of plate active area (mm)
k	mass transfer coefficient (mm/s)
n	number of electrons transferred in the reaction
Re_v	vibrational Reynolds number ($Re_v = a\omega L/v$)
S	shear rate at the solid–liquid interface (s^{-1})
Sc	Schmidt number, ($Sc = \nu/D$)
Sh	Sherwood Number, ($Sh = kL/D$)
t	time (s)
u	x-directional velocity (mm/s)
V	y-directional velocity (mm/s)
x	positions along the flat plate (mm)
y	positions normal to the flat plate (mm)
$\breve{y}$	centre of mass, Eq. (37) (mm)

Greek symbols

α	specific densification coefficient (mm^3/mol)
β,γ	coefficient of expansion, Eq. (18)
ν	kinematic viscosity (mm^2/s)
ρ	fluid density (g/mm^3)
ω	circular frequency of vibration, $2\pi f$ (s^{-1})
ϕ	dimensionless concentration [$\phi = (c_0 - c)/c_0$]
η	dimensionless Polhausen variable, Eq. (9)
ψ	stream function, Eq. (10)
ξ	similarity variable, Eq. (26)
Γ	gamma function

Subscripts

f	forced convection
n	natural convection
o	conditions outside the boundary layer
s	condition at the plate surface
v	time average vibrational value

development of effective scale up methodologies. For example, mass transfer enhancement due to the formation of turbulent eddies is significantly different from that caused by acoustic streaming, or boundary layer thinning, and the parameters affecting each are also different [23,24]. This issue is of major concern from a reactor engineering point of view since various applications place different emphasis on various mechanisms. For example, while overcoming surface fouling in membrane filtration is best achieved under conditions where turbulent eddies and vortices are generated along the solid–fluid interface, minimizing concentration polarization and thinning of the diffusion boundary layer would be more desired to in an electrochemical reactor design. Another example, where lack of proper understanding of such an issue has resulted in disagreement between the various investigators, is the effect of oscillatory flow on performance improvement, where some authors attribute it to standing vortex wave formation [25,26], while others reported that much of it, if not most, is due to the negative pressure portion generated each half cycle of the oscillatory cycle [27,28], and both mechanisms, on the other hand are different from enhancement due to self-sustained resonant transport [29]. Proper understanding of the enhancement mechanism is therefore necessary in order to allow for the development of proper scaleup methodologies and for achieving the full potential of using oscillatory motion for improving performance of processes hindered by diffusion-limitation and surface fouling, such as membrane separation and electrochemical applications.

In this paper an analytical model is developed to explain the effect of oscillatory motion on both fluid mechanics and mass transfer, which vary with periodicity in both time and space at vertical solid–fluid interface. It will also provide basis for modeling of more complex systems such as oscillatory flows in presence of turbulence promoters, and measurement of wall shear at vertical surfaces under oscillatory flow conditions using mass transfer measurements technique. The mass transfer characteristics are discussed with reference to the velocity and concentration distributions, and the mixed convection phenomena induced by the buoyancy effect is discussed. The model predictions are compared with experimental measurements of Gomaa et al. [4], as well as other investigators.

2. Theortical analysis

2.1. Background

The subject of diffusion across unsteady boundary layer has been addressed by several investigators [31–39] where it was demonstrated that under conditions of slow shear variation (low frequencies), a quasi-steady assumption can be made and Leveque's one-third-power law [30], in which the flux is proportional to the one-third power of the local shear rate, can be used. In cases, where the variation of the shear rate is fast (high frequencies), significant deviation from the quasi-steady state predictions occurs, and knowledge of the dynamic behavior of the concentration boundary layer is required. This was analyzed for small amplitude oscillations, where the boundary layer equation can be linearized and solved asymptotically or numerically. For large amplitude oscillations where shear reversal occurs, the basic simplification of the boundary-layer theory is lost since the "leading edge" of the body changes ends, and the velocity profile

at a given point along the surface becomes not only dependent on the upstream, but also on the downstream flow conditions at different times. For such conditions, Pedley [40] developed a model based on combining an asymptotic quasi steady expansion solution with a purely diffusive one during shear reversal that fairly predicted experimental results. The basis of the analysis was also confirmed by Watkins and Herron [41] who showed that for a plate oscillating with a zero mean velocity, a Stokes layer will exist over the plate surface except for a small distance from its leading edge. The problem was also analyzed by Kaiping [42], Steenhoven et al. [43], and Mao and Hanratty [44,45], who examined numerically the unsteady forced convective transfer under reversing shear flow conditions, and reported similar results.

In presence of natural convection, the situation is more complex due to the coupling of the mass and momentum equations, and most investigations focused on experimentally developed correlations for the time-average transfer component [46–48]. Analytical solutions of the dynamic behavior were limited to either cases of small amplitude oscillation [49–51], or bodies of revolution [52–54].

Recently, Gomaa et al. [4] measured both the transient and time average mass transfer rates at a vertically oscillating flat plates using the limiting current technique. Their results showed a definite oscillatory mass transfer component (AC) superimposed on a much larger steady one (DC) throughout the vibratory cycle. Similar observations were also reported by Liu et al. [46] mass transfer measurements at vertically oscillating electrodes, where the AC component showed relatively little changes throughout the vibratory cycle, and did not follow the oscillatory velocity, which periodically approaches zero at reversal times. Although the above authors successfully correlated the time-average transfer rates using quasi-steady state approach in which the plate average vibrational velocity was used as the stream velocity, the approach failed to describe its transient behavior and its interaction with free convection.

2.2. Model development

Consider the vertical thin flat plate in Fig. 1 where a fully developed steady state natural convection is established due to density difference as in the case of a stationary electrode under limiting current conditions. As the plate oscillates harmonically in its own plane, and away from its leading edge, a new layer (Stokes layer) carried by the plate will develop, which is much thinner than the original natural convection layer, and diffusion across such layer will amplify the natural convection process resulting in the higher DC mass transfer component. Near the plate leading edge, on the other hand, a quasi-steady state forced convection mechanism is dominant and extends from the active plate leading edge to a point on the surface when a particle that past the surface active leading edge first arrive at that point before the plate changes direction. This mechanism is periodic, and will contribute to the AC mass transfer component. In other words,

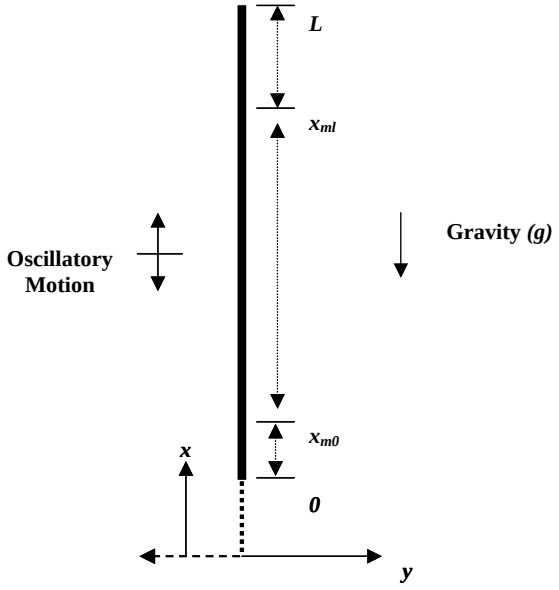

Fig. 1. Schematic of analytical model.

for points on the surface that are never reached by fluid particles, or the fluid velocity there is too small, as is the case near shear reversal, the quasi-steady solution is replaced by diffusive solution in presence of gravity.

Based on the above assumptions, and assuming that the property variation with concentration is limited to density and its effects on the buoyancy term in the momentum equation (Boussinesq approximation), the continuity, momentum, and diffusion equations with their appropriate boundary conditions with respect to a reference frame fixed to the oscillating plate, are given by:

$$\frac{\partial u}{\partial x} + \frac{\partial v}{\partial y} = 0 \tag{1}$$

$$\frac{\partial u}{\partial t} + u\frac{\partial u}{\partial x} + v\frac{\partial u}{\partial y} = v\frac{\partial^2 u}{\partial y^2} + \frac{g(\rho(c_0) - \rho(c))}{\rho(c)} + \frac{\mathrm{d}u_0}{\mathrm{d}t} \tag{2}$$

$$\frac{\partial c}{\partial t} + u\frac{\partial c}{\partial x} + v\frac{\partial c}{\partial y} = D\frac{\partial^2 c}{\partial y^2} \tag{3}$$

where u_0 is the fluid velocity outside the boundary layer relative to the selected coordinate axis, given by;

$$u_0 = a\omega\cos(\omega t) \tag{4}$$

and the boundary conditions given by:

$$u(x, 0, t) = v(x, 0, t) = 0 \tag{5a}$$

$$u(x, \infty, t) = u_0 \tag{5b}$$

$$c(x, 0, t) = c_s = 0 \tag{5c}$$

$$c(x, \infty, t) = c_0 \tag{5d}$$

The above boundary conditions correspond to the limiting current condition where the concentration of the active species vanishes at the wall, (i.e. $c_s = 0$).

Since boundary layer linearization cannot be applied in cases involving shear reversal, a solution will be developed near the plate leading edge based on the fact that, the flow there is essentially Blasius, and the situation is that of determining the effect of the buoyancy forces on the upward or downward forced convection solution. On the other hand, and far away from the plate leading edge, the layer is mainly Stokes, and the situation will be of determining the rate of diffusion across the layer in presence of buoyancy force.

2.3. Development of the pseudo-steady state solution (DC)

Away from the plate leading edge, and as the plate starts to oscillate, an unsteady problem is formed that eventually evolves to the well known Stokes flow conditions at large times [55]. The intent is to evaluate the effect of oscillations on the steady state solution without residing to solving the initial value problem. In doing so the steady state mass and momentum equations will be used, and Eqs. (2)–(3) reduce to:

$$u\frac{\partial u}{\partial x} + v\frac{\partial u}{\partial y} = \nu\frac{\partial^2 u}{\partial y^2} + g\alpha\phi \tag{6}$$

$$u\frac{\partial c}{\partial x} + v\frac{\partial c}{\partial y} = D\frac{\partial^2 c}{\partial y^2} \tag{7}$$

where, ϕ is the dimensionless concentration defined by: $\phi = (c_0 - c)/c_0$, and α, the specific densification coefficient

$$\alpha = \frac{c_0}{\rho(c_0)}\left[\frac{\partial \rho}{\partial c}\right]_{c=c_0} \tag{8}$$

introducing the dimensionless Pohlhausen variable,

$$\eta = \left[\frac{g\alpha}{4\nu^2}\right]^{1/4}\frac{y}{x^{1/4}} \tag{9}$$

and the stream function

$$\Psi = 4\nu\left[\frac{g\alpha}{4\nu^2}\right]^{1/4} x^{3/4} h(\eta) \tag{10}$$

where the function h is still unknown. In terms of the new variable, the velocity components,

$$u = 4\nu\left[\frac{g\alpha}{4\nu^2}\right]^{1/2} h'(\eta), \tag{11}$$

$$v = \nu\left[\frac{g\alpha}{4\nu^2}\right]^{1/4}\frac{(\eta h' - 3h)}{x^{1/4}} \tag{11a}$$

and Eqs. (6) and (7) take the form:

$$h''' + 3hh'' - 2(h')^2 + \varphi = 0 \tag{12}$$

$$\varphi'' + 3Sch\varphi' = 0 \tag{13}$$

and, finally, for the boundary conditions of the problem, we obtain the expressions

$$h = h' = 0, \quad \varphi = 1, \quad \text{for } \eta = 0 \tag{14}$$

$$h' = h_0, \quad \varphi = 0 \quad \text{for } \eta = \infty \tag{15}$$

In the case of liquids, Sc number is very large, and the solution of Eq. (13) takes the following form

$$\varphi = 1 - \frac{\left[\int_0^\eta \exp\left\{-3Sc\int_0^\eta h\,\mathrm{d}\eta\right\}\mathrm{d}\eta\right]}{\left[\int_0^\infty \exp\left\{-3Sc\int_0^\eta h\,\mathrm{d}\eta\right\}\,\mathrm{d}\eta\right]} \tag{16}$$

In Eq. (16), the function h would be determined based on the fact that the integrals converge very rapidly due to the large values of Sc number, and its magnitude is determined mainly by the value of h for small values of η. Therefore, and without introducing any significant error, the boundary conditions at infinity given in Eq. (15) may be replaced by new boundary conditions, which is fulfilled at a finite distance $\eta = \eta_0$ from the surface

$$h' = \frac{u(\eta_0)}{4\nu[g\alpha/4\nu^2]^{1/2}} \tag{17a}$$

$$\varphi = 0, \quad \eta = \eta_0 \tag{17b}$$

and $u(\eta_0)$ and η_0 are given by [55],

$$u(\eta_0) = aw\{1 - e_0^{-\eta}\cos(wt - \eta_0)\} \tag{17c}$$

$$\eta_0 = y_0\left(\frac{w}{2\nu}\right)^{1/2} \tag{17d}$$

Owing to the rapid convergence of the integrals in Eq. (16), we can write a series expansion in powers of η for the function h for $\eta < \eta_0$, and retain only the first terms of the expansion. In view of the boundary conditions in Eq. (14), the series expansion of h is

$$h = \left(\frac{\beta}{2}\right)\eta^2 + \left(\frac{\gamma}{6}\right)\eta^3 + \cdots\cdots \tag{18}$$

substituting the expression for h from Eq. (18) into the solution given in Eq. (16), and using only one term as first approximation

$$\varphi = 1 - \frac{\left[\int_0^\eta \exp\left\{-\beta Sc(\eta^3/2)\right\}\mathrm{d}\eta\right]}{\left[\int_0^\infty \exp\left\{-\beta Sc(\eta^3/2)\right\}\mathrm{d}\eta\right]} \tag{19}$$

which yields the following solution:

$$\varphi \approx 1 - \frac{[(\beta Sc/2)^{1/3}\eta]}{\Gamma(4/3)} \tag{20}$$

using the boundary conditions in (17b)

$$\varphi = 0 \approx 1 - \frac{[(\beta Sc/2)^{1/3}\eta_0]}{\Gamma(4/3)} \tag{21}$$

substituting the concentration distribution given by Eq. (20) into Eq. (12)

$$h''' + 3hh'' - 2(h')^2 + 1 - \frac{[(\beta Sc/2)^{1/3}\eta]}{\Gamma(4/3)} = 0 \tag{22}$$

using the method of successive approximation, and restricting the solution to the lower powers of η, an approximate solution of (22), may be written in the form

$$h = \frac{\beta\eta^2}{2} - \frac{\eta^3}{6} + \frac{[(\beta Sc/2)^{1/3}\eta^4]}{[(24)\Gamma(4/3)]} \tag{23}$$

from the boundary condition in (17a),

$$\beta\eta_0 - \frac{\eta_0^2}{2} + \frac{[(\beta Sc/2)^{1/3}\eta_0^3]}{[(6)\Gamma(4/3)]} - \frac{u(\eta_0)}{[4\nu[g\alpha/4\nu^2]^{1/2}]} = 0 \quad (24)$$

solving (24) with (21), and reverting to dimensional variables, the concentration distribution can be determined using Eq. (20) in the form

$$c = c_0 \left(\frac{\beta Sc}{2}\right)^{1/3} \left[\frac{g\alpha}{4\nu^2}\right]^{1/4} \frac{y}{x^{1/4}} \quad (25)$$

2.4. Solution near the leading active edge (oscillatory-AC component)

The oscillatory solution will be determined, for simplicity, for one cycle oscillation, where the plate reverse its direction at time $t = 0$. For a point x on the surface, and long before reversal, fluid velocity, and consequently the convection term, are large in comparison with unsteady diffusion, and the concentration distribution can be approximated by a "quasi-steady" solution. This condition will continue until a time $-t_1(x)$ when fluid particles which had passed the leading edge at $x = 0$ first failed to arrive at x before flow reversal. For $t > -t_1(x)$, the fluid velocity is too small to an extend where convection becomes relatively unimportant, and the concentration distribution can be approximated by a "quasi-diffusive" solution. This condition will continue through shear reversal until time $t_2(x)$ when the fluid velocity becomes sufficiently large again, and a quasi-steady layer growing from the opposite edge at $x = L$ arrives at point x, and a quasi-steady solution is applied again. If conditions are such that no fluid particles arrives to x from L, then the quasi-diffusive solution will proceed through the second reversal until a quasi-steady layer reaches x from $x = 0$ again. For that part of the surface where the effect of neither edge is felt, the concentration distribution will be given by the steady solution in Eq. (25). Applying the above assumptions:

2.4.1. For times $t < -t_1(x)$, and $t > t_2(x)$

Which represents times long before and after shear reversal, Eq. (3), can be solved by omitting the unsteady term, and approximating the velocity by the sum of its oscillatory and natural convection components. Introducing the similarity variable ξ,

$$\xi = y\left[\frac{S^{1/2}}{(9D\int_0^x S^{1/2}\,\mathrm{d}x)}\right]^{1/3} \quad (26)$$

Eq. (3) can be written as

$$\varphi'' + 3\xi^2\varphi' = 0 \quad (27)$$

where,

$$u = yS, \quad v = -\left(\frac{1}{2}\right) y^2 S' \quad (28)$$

$$S = S_f + S_n = \left(\frac{\partial u}{\partial y}\right)_{y=0} \quad (29)$$

$$S_f = a\omega^{3/2}\frac{\cos(\omega t + (\pi/4))}{\nu^{1/2}} \quad (30)$$

$$S_n = 4\beta\nu\left[\frac{g\alpha}{4\nu^2}\right]^{3/4} x^{1/4} \quad (31)$$

and the resulting solution leads to:

$$c = c_0\left\{1 - \left[\frac{1}{\Gamma(4/3)}\right]\int_0^{\xi} e^{-\xi^3}\,\mathrm{d}\xi\right\} \quad (32)$$

2.4.2. For times $-t_1(x) < t < t_2(x)$

Which represent the period near shear reversal, the convective term in Eq. (3) becomes small and the concentration distribution is given by the lateral unsteady diffusion

$$\frac{\partial c}{\partial t} = D\frac{\partial^2 c}{\partial y^2} \quad (33)$$

The appropriate solution of (33) is

$$c = c_0 erfc\{y[4D(t(x) + t_i(x))]^{-1/2}\} \quad (34)$$

where t_i (x) is the initial conditions required to solve (33), and represents the time when pure diffusion has started or the "virtual origin of the diffusion". Eqs. (32) and (34) can be used for determining the oscillatory mass transfer component by determining the transition times, $-t_1(x)$, $t_i(x)$, and $t_2(x)$ together with maximum penetration distance, or the leading edge effect. The latter is determined from

$$x_{m0} = y\int_{-\pi/\omega}^{0} S\,\mathrm{d}t \quad \text{for } -\frac{\pi}{\omega} < t < 0 \quad (35)$$

and,

$$x_{ml} = y\int_{0}^{\pi/\omega} S\,\mathrm{d}t \quad \text{for } 0 < t < \frac{\pi}{\omega} \quad (36)$$

since u is sheared proportional to y and does not take a unique value, the criteria proposed by Pedley [40] for selecting the

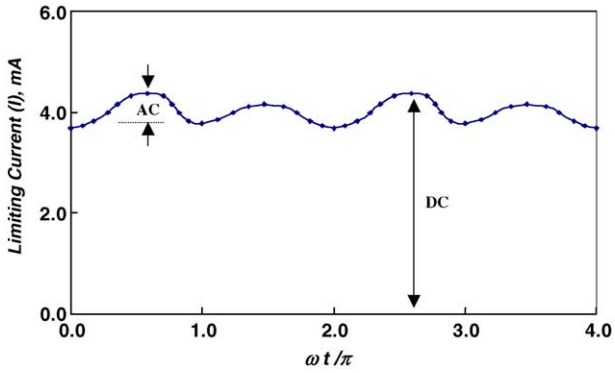

Fig. 2. Transient behavior of the limiting current ($a = 20$ mm, $f = 5$ Hz, $L = 3$ mm).

value of y at the center of mass will be applied. The center of mass $\breve{y}$ is defined by

$$\breve{y} = \frac{\int_0^\infty yc\,\mathrm{d}y}{\int_0^\infty c\,\mathrm{d}y} \tag{37}$$

which is determined from Eq. (32),

$$\breve{y} = 0.37\left[\frac{9Dx}{S(t)}\right]^{1/3} \tag{38}$$

The time parameters $-t_1(x)$ and $t_2(x)$ are determined by solving Eqs. (35) and (36) for each point on the surface,

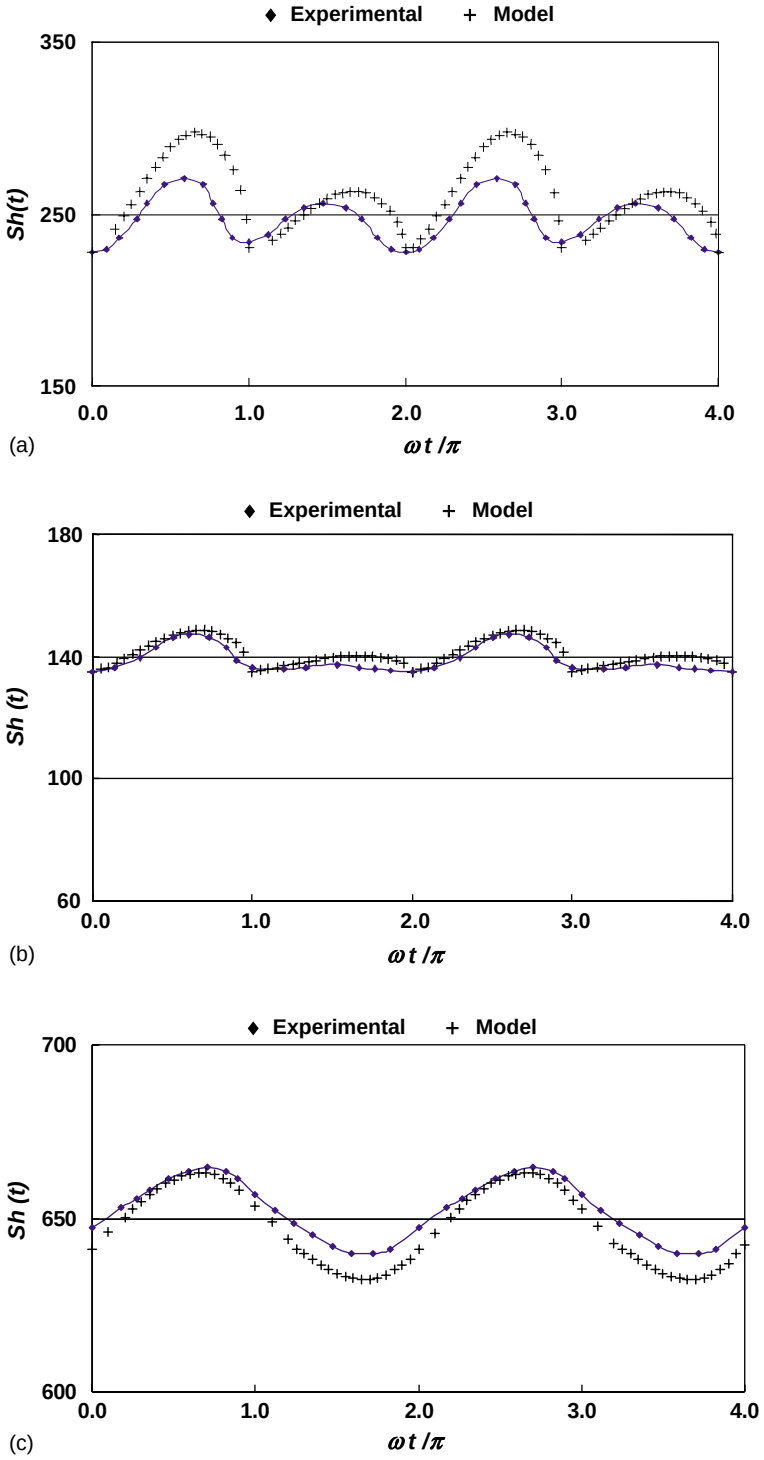

Fig. 3. Oscillatory mass transfer. Comparison of model and experimental data. (a) $a = 20$ mm, $f = 5$ Hz, $L = 3$ mm; (b) $a = 5$ mm, $f = 3$ Hz, $L = 5$ mm; (c) $a = 5$ mm, $f = 5$ Hz, $L = 130$ mm.

say x_T, where there is a transition between the quasi-steady and diffusive solution in the range $0 < x < x_{m0}$, and $(L - x_{ml}) < x < x_{ml}$. The virtual origin of diffusion $t_i(x)$, is determined by the requirement that the center of mass of the concentration distribution be continuous at the transition time. From Eqs. (32) and (34), continuity of this quantity requires that,

$$\left(\frac{\pi}{4}\right)(t_0(x) - t_1(x)) = \left[\frac{9Dx}{S(-t_1(x))}\right]^{2/3} \xi^{2\prime} \tag{39}$$

the overall time dependent mass transfer coefficient can then be determined from

$$k(t) = \left(\frac{D}{c_0 L}\right)\int_0^L \left[-\frac{\partial c}{\partial y}\right]_{y=0} \mathrm{d}x \tag{40}$$

where the integrand is given by the solutions in Eqs. (25), (32), and (34) to be:

$$\left[-\frac{\partial c}{\partial y}\right]_{y=0} = c_0 \frac{[-S(t)/9Dx]^{1/3}}{\Gamma(4/3)} \quad \text{for } t \le -t_1 \tag{41a}$$

$$\left[-\frac{\partial c}{\partial y}\right]_{y=0} = c_0 \frac{[-S(t)/9D(1-x)]^{1/3}}{\Gamma(4/3)} \quad \text{for } t \ge t_2 \tag{41b}$$

$$\left[-\frac{\partial c}{\partial y}\right]_{y=0} = c_0[\pi D(t_0(x)+t_1(x))]^{-1/2} \quad \text{for } -t_1 < t < t_2 \tag{41c}$$

$$\left[-\frac{\partial c}{\partial y}\right]_{y=0} = c_0\left(\frac{\beta Sc}{2}\right)^{1/3} \frac{[g\alpha/4\nu^2]^{1/4}}{x^{1/4}} \quad \text{for all } t, x_{m0}, < x < x_{ml} \tag{41d}$$

$k(t)$ is evaluated by integrating either (41a) from 0 to x_T and (41c) from x_T to L, if $S(t) > 0$, or (41c) from 0 to x_T and (41b) from x_T to L, if $S(t) < 0$. If conditions are such that there exist a section on the surface $x_{m0}, < x < x_{ml}$ where the effect of neither leading edges is felt, then Eq. (41d) will be integrated from x_{m0}, to x_{ml}, for the entire cycle to determine the steady state component. The oscillatory component in this case is evaluated by integrating either (41a) from 0 to x_T and (41c) from x_T to x_{m0}, and from x_{ml} to L if $S(t) > 0$, or (41c) from 0 to x_{m0} and from x_{ml} to x_T and (41b) from x_T to L, if $S(t) < 0$. The overall time average mass transfer coefficient is then determined from

$$k_v = \left(\frac{1}{2\pi}\right)\int_{-\pi/\omega}^{\pi/\omega} k(t)\,\mathrm{d}t \tag{42}$$

3. Results and discussion

To validate the proposed analysis, both the transient and time average mass transfer coefficient at vertically oscillating flat surfaces were measured for a wide range of frequencies, amplitudes, and surface heights using the limiting current technique (a = 0–20 mm, f = 0–25 Hz, L = 3–130 mm) This corresponds to $2.8 \times 10^5 < Gr \times Sc < 1.86 \times 10^{10}$. Details of the experimental setup and method of calculation were given by Gomaa et al. [4]. The measurements were conducted using nickel electrodes embedded into a carrier plate to ensure absence of surface deformity and eliminate streaming and eddy generation at the leading edge. The system potassium ferri-ferrocyanide in aqueous sodium hydroxide solution was selected in order to accurately monitor rapid variations in mass transfer rates. Under limiting current conditions, the concentration of the ferricyanide is reduced to zero at the cathode, and the mass transfer coefficient, k, is calculated from

$$k = \frac{I_L}{AnFc_0} \tag{43}$$

3.1. Oscillatory mass transfer

Analysis of the transient limiting current data revealed several observations that could not be explained by the quasi-steady analysis. First, and as shown in Fig. 2, the oscillatory component, is relatively small in comparison to the steady component, with the AC/DC decreasing with increasing L/a, as seen in Figs. 3 and 4. The present model fairly predicts and explains such observations, where the presence of a quasi-diffusive mechanism accounts for the relatively large DC component. It also explains the effect of L/a on AC/DC ratio since the latter is determined by the fraction of surface being reached by fluid particles from the plate leading edge each half cycle, which increases with the amplitude of oscillation.

The second observation is the complex harmonic structure of the oscillatory component, which behaved as a composite signal of two sub-harmonics with characteristic frequencies f and $2f$ that varied in amplitude depending on the surface height and its vibrational parameters. For example, while the amplitude of the second harmonic in Fig. 3a is ~67% of the first, it decreases as L/a increases to ~23% in Fig. 3b, and almost vanishes to a single harmonic per cycle at higher L/a, as shown in Fig. 3c. In light of the present analysis, this can be attributed to the opposite effect of the buoyancy force in each half of the oscillating cycle, which increases with

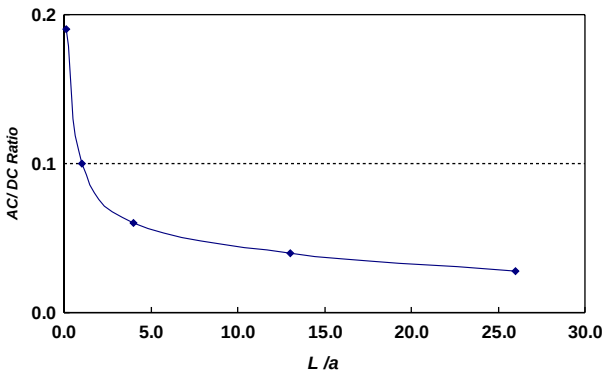

Fig. 4. Effect of L/a on the AC/DC ratio.

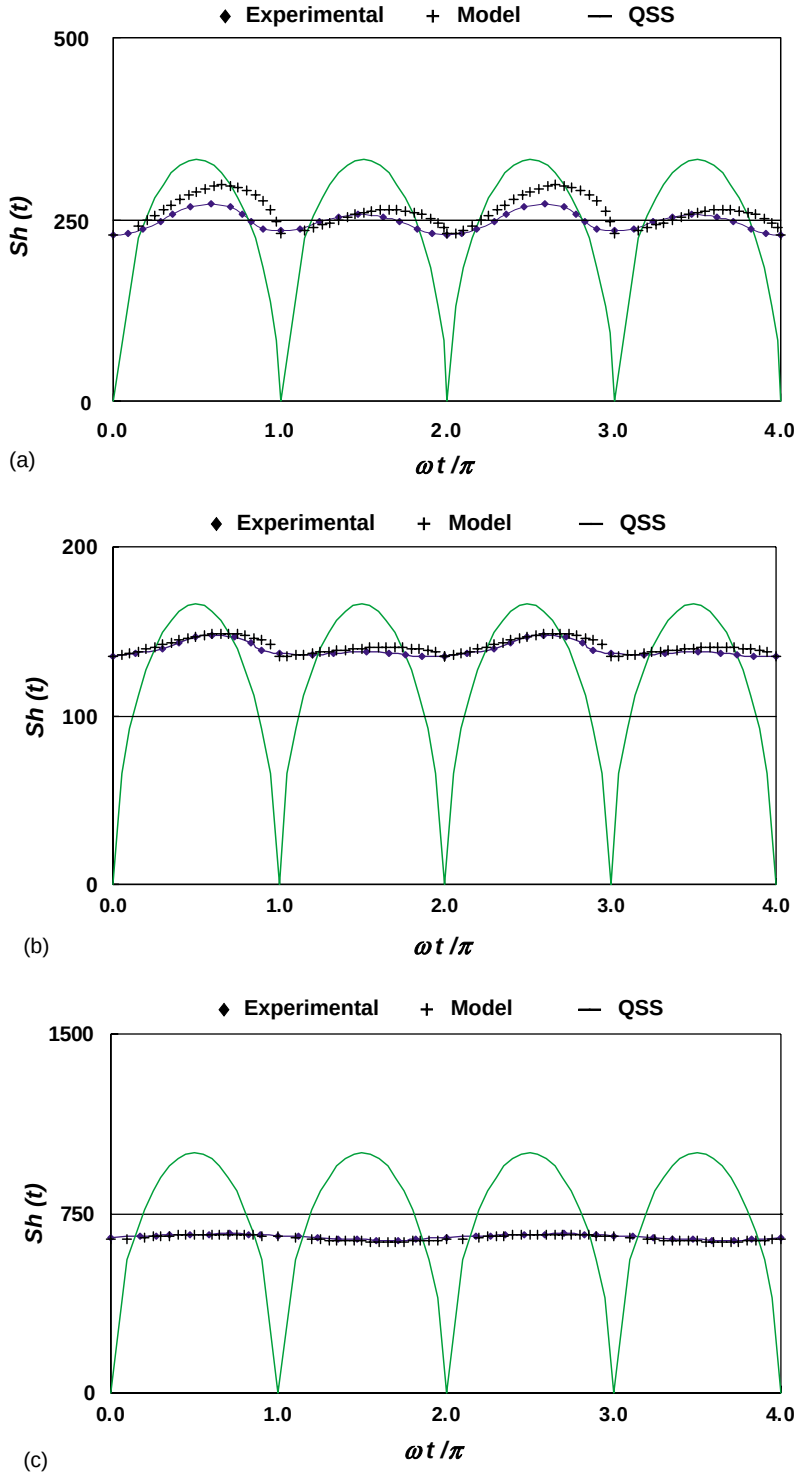

Fig. 5. Oscillatory mass transfer. Comparison of model and quasi-steady analysis. (a) $a = 20\,\text{mm}$, $f = 5\,\text{Hz}$, $L = 3\,\text{mm}$; (b) $a = 5\,\text{mm}$, $f = 3\,\text{Hz}$, $L = 5\,\text{mm}$; (c) $a = 5\,\text{mm}$, $f = 5\,\text{Hz}$, $L = 130\,\text{mm}$.

L/a until a situation occurs where the steady effect becomes much higher than the oscillatory term to prevent any shear reversal and the formation of a second harmonic during the second half of the cycle.

As can be seen from Fig. 5, the present analysis agrees with the experimental data, especially during flow acceleration, and also adequately describes the mass flux plateau which differs completely from Leveque solution, which contains only oscillatory component of a magnitude that varies between zero and a maximum that is ∼35% higher than the average. The agreement however seems to be highest at larger L/a ratios, as can be seen from Fig. 3 where the

maximum deviation is ~10% at $L/a = 0.15$, and reduces to ~6% for $L/a = 1$ and ~2% for $L/a = 26$. Such behavior can be attributed in part to the increased influence of the leading edge at higher amplitude to surface ratios, which would increase the associated error resulting from the "abrupt take-over" assumption between the quasi-steady and diffusive mechanisms near reversal times. Another factor which would also contribute to the higher deviation, is the effect of the "so-called wake", where a relatively low concentration fluid is carried back over the surface during reversal time, a factor that was not addressed in the present analysis, and could become more significant (at larger) for smaller L/a ratios.

3.2. Time average mass transfer coefficient

The rate of mass transfer at the surface of stationary vertical plates is controlled by diffusion through natural convection boundary layer created by the density difference between the reactants and products at its surface. When the plates were vibrated, the average current density, and subsequently the time average vibrational mass transfer coefficient (k_v), was found to increase substantially with increasing either the frequency or amplitude of vibration, with the extent of enhancement being most pronounced at small heights. This increase, as explained earlier, is attributed to the thinning of the boundary layer over the surface, combined with the enhanced transfer at the plate active mass transfer area leading edges, which also increases with both amplitude and frequency of vibration. It is clear from Fig. 6a and b that the model predictions agrees fairly well with the experimental measurements of Gomaa et al. [4]. It also agrees with the data of Liu et al. [46], who used smaller amplitudes and higher frequencies in a different system (copper sulfate, sulfuric acid), as can be seen from Fig. 7a and b. Furthermore, the applicability of the model extends for a wide range of operating conditions since it converges to the pure natural convection solution as $aw \to 0$, and to pure oscillatory forced convection in absence of buoyancy force. In the first case, $h' \to 0$ in Eq. (17a) and the average mass transfer coefficient is calculated by integrating Eq. (41d) over the entire surface, which leads to the standard natural convection

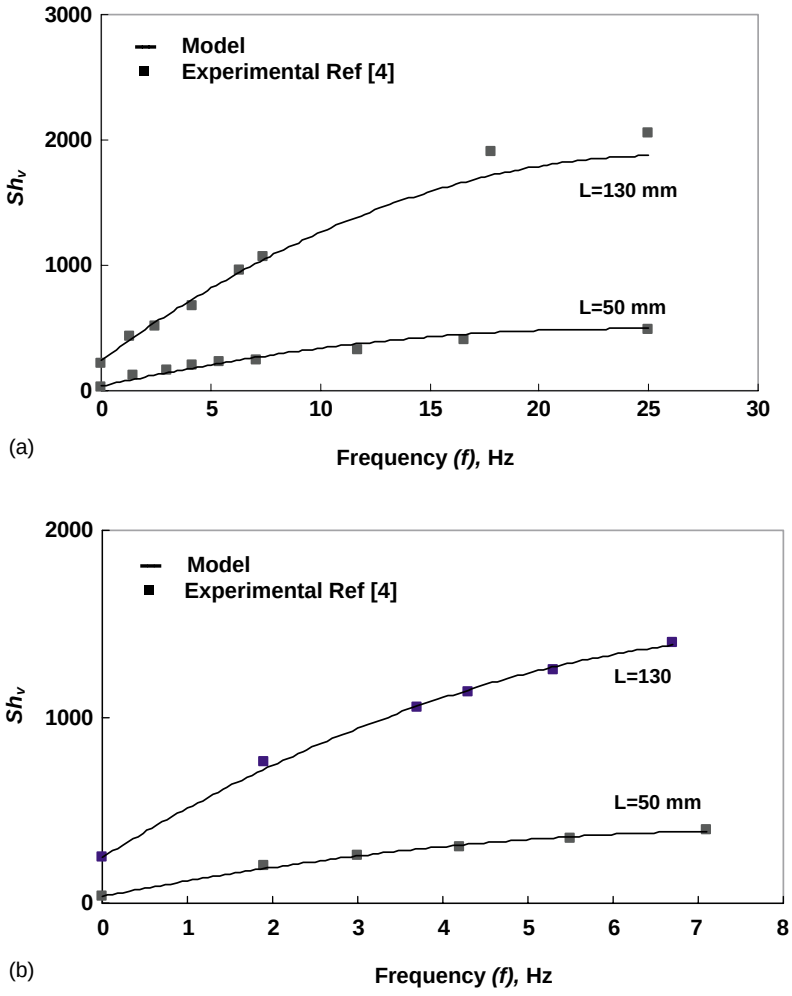

Fig. 6. Effect of frequency on Sh_v Ref. [4]. (a) $a = 5$ mm; (b) $a = 10$ mm.

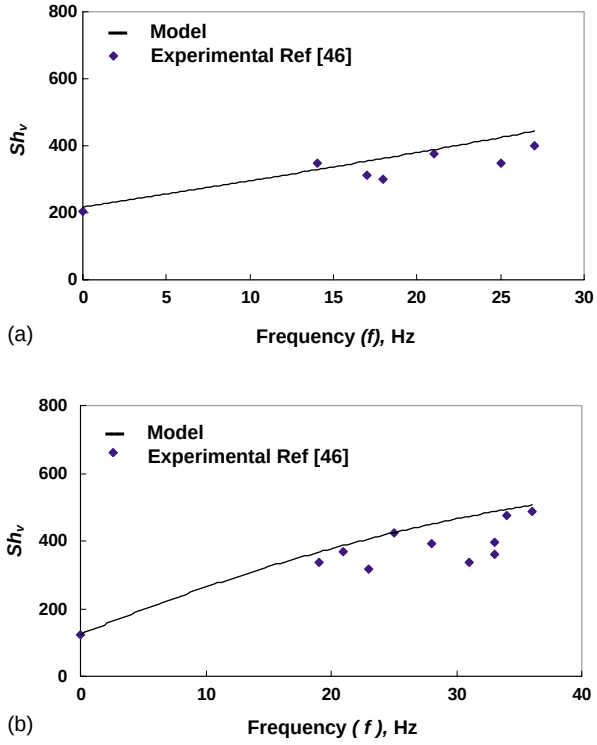

Fig. 7. Effect of frequency on Sh_v Ref. [46]. (a) $a = 0.057$ mm, $L = 50.8$ mm; (b) $a = 1.14$ mm, $L = 25.4$ mm.

solution [55],

$$Sh_n = 0.67(Gr \times Sc)^{0.25} \quad (44)$$

In the second case, Eq. (41d) $\rightarrow 0$, and since the dynamic behavior of the mass transfer component is not required, Eq. (41c) can be substituted by either Eq. (41a) or Eq. (41b), which in absence of natural convection give the same time average value for both halves of the oscillatory cycle. The time average mass transfer coefficient is then calculated by integrating either equation over the entire surface using a time average expression for the vibrational velocity ($u_{ave} = 0.64a\omega$) to give the standard equation for mass transfer over a flat plate given by [55],

$$Sh_f = 0.67Re^{0.5}Sc^{0.333} \quad (45)$$

Eq. (45) can also be written in terms of the vibrational Reynolds number $Re_v = awL/v$,

$$Sh_f = 0.52Re_v^{0.5}Sc^{0.333} \quad (45a)$$

the above observations suggest that it is possible from a practical point of view to express the effect of oscillation on mass transfer at vertical surface in terms of mixed natural and forced convections, and to estimate Sh_v using a mixed convection correlation given by [56],

$$Sh_v = [Sh_n^3 + Sh_f^3]^{1/3} \quad (46)$$

Fig. 8 shows the mass transfer results calculated using both the present model and Eq. (46), plotted in terms of the dimensionless ratio $Gr/Re^2Sc^{1/3}$, which according to Acrivos [57] determines the relative contribution of forced and natural convection, with forced convection prevailing if $Gr/Re^2Sc^{1/3}$ is <0.1. As can be seen from Fig. 8, Eq. (46) agrees fairly well with the present model, as well as the experimental data of both Gomaa et al. [4], (107 points), as well as those of Liu et al. [46], (47 points). This further support the proposal of using mixed convection correlation for predicting the effect of oscillation on the time average mass transfer at vertical surfaces. It also explains the success in correlating the experimental data by above authors using forced convection correlations, since most of their data lay in the region where $Gr/Re^2Sc^{1/3}$ is <0.1. The general comparison given in Fig. 9 shows that the entire set of experimental data of the above authors were satisfactorily correlated using Eq. (46) with correlation coefficient $R = 0.98$.

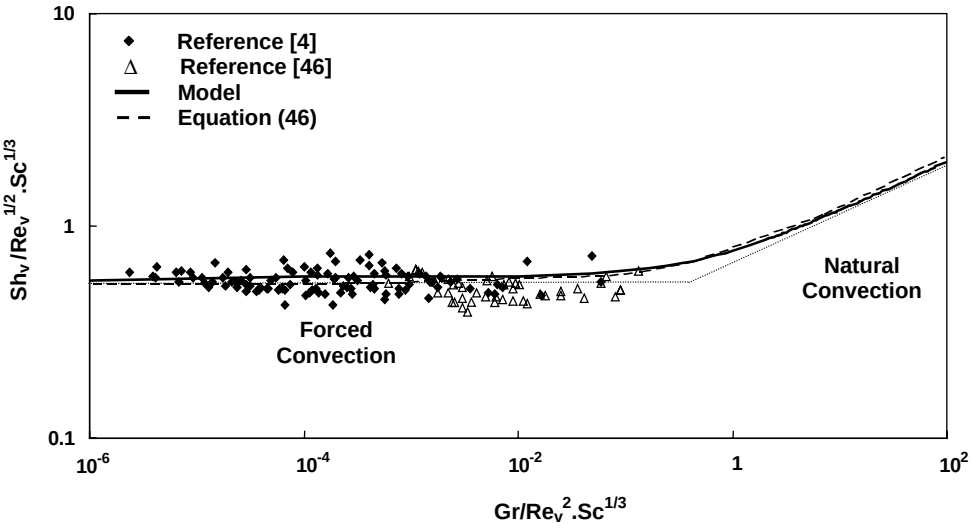

Fig. 8. Comparison between model and NC, and FC convection equations.

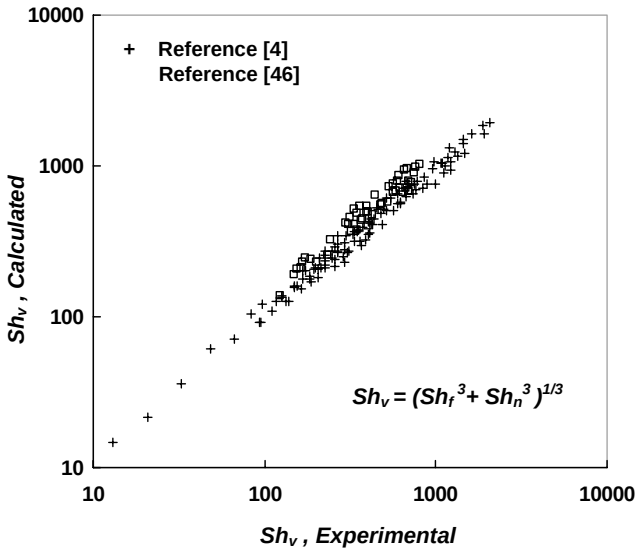

Fig. 9. Comparison between Eq. (46) and experimental data, Refs. [4,46].

4. Conclusions

The rate of mass transfer at vertical plates increases substantially when the plates are vibrated parallel to their surfaces with the increase being highest at high frequencies and amplitude of vibration. The enhancement can be attributed to two mass transfer mechanisms. First, and away from the plate active leading edge, mass transfer occurs primarily by diffusion across the layer carried by the plate (Stokes layer), which is much thinner than natural convection layer in absence of oscillation. Second, and near the plate active leading edge, a quasi-steady mechanism is dominant and contributes to the formation of an AC component with characteristic frequency that varies in amplitude and frequency from f for large values of L/a to $2f$, with increasing the amplitude to height ratio. The model predicts both the time average and dynamic behavior of the mass flux, with the degree of accuracy being highest at large L/a ratios. From a practical point of view, it is possible to calculate the time average mass transfer coefficient using a mixed convection expression with the forced convection term calculated based on the time average vibrational velocity of the oscillating surface.

References

[1] X. Ni, M.R. Mackley, A.P. Harvey, P. Stonestreet, M.H.I. Baird, N.V. Rama Rao, Mixing through oscillations and pulsations: a guide to achieve process enhancements in the chemical and process industries, Trans. Inst. Chem. Eng. 81 (2003) 373–383.

[2] M.E. Mackay, M.R. Mackley, Y. Wang, Oscillatory flow within tubes containing wall or central baffles, Trans. Inst. Chem. Eng. 69 (1991) 506.

[3] P. Gao, W. Han Ching, M. Herrmann, C. Kwong, P.L. Yue, Photo-oxidation of a model pollutant in an oscillatory flow reactor with baffles, Chem. Eng. Sci. 58 (3-6) (2003) 1013–1021.

[4] H.G. Gomaa, A.M. Al-Taweel, J. Landau, Mass transfer enhancement at vertically oscillating electrodes, Chem. Eng. J. 97 (2004) 141–149.

[5] M.B. Liu, G.M. Cook, N.P. Yao, Vibrating zinc electrodes in Ni/Zn batteries, J. Electrochem. Soc. 129 (1982) 913–920.

[6] A.M. Thomas, R. Narayanan, A comparison between mass transfer in boundary and pressure driven oscillatory flow, Int. J. Heat Mass Transfer 45 (2002) 4057–4062.

[7] V. Perez-Herranz, J. Garcia-Anton, J.L. Guinon, Velocity profiles and limiting current in an electrodialysis cell in pulsed flow, Chem. Eng. Sci. 52 (5) (1997) 843–851.

[8] A.K. Chandhok, D.T. Leighton, Oscillatory cross-flow electrophoresis, AIChE J. 37 (10) (1991) 1537–1549.

[9] S. Najarian, B.J. Bellhouse, Effect of oscillatory flow on the performance of a novel cross-flow affinity membrane device, Biotech. Prog. 13 (1997) 113–116.

[10] P. Blanpain-Avet, N. Doubrovine, C. Lafforgue, M. Lalande, The effect of oscillatory flow on cross-flow microfiltration of beer in a tubular mineral membrane system–membrane fouling resistance decrease and energetic considerations, J. Mem. Sci. 152 (1999) 151–174.

[11] W.B. Krantz, R.R. Bilodeau, M.E. Voorhees, R.J. Elgas, Use of axial membrane vibration to enhance mass transfer hollow tube oxygenator, J. Mem. Sci. 124 (1997) 283.

[12] B.J. Bellhouse, R.W. Lewis, A high efficiency membrane separator for donor plasmapheresis, Trans. Am. Soc. Artif. Intern. Organs. 34 (1988) 747–754.

[13] H. Nagaoka, Mass transfer mechanism in biofilms under oscillatory flow conditions, Wat. Sci. Tech. 36 (1) (1997) 329–336.

[14] S. Beeton, H.R. Millward, B.J. Bellhouse, A.M. Nicholson, N. Jenkins, C.J. Knowles, Gas transfer characteristics of a novel membrane bioreactor, Biotech. Bioeng. 38 (1991) 1233–1238.

[15] H.R. Millward, B.J. Bellhouse, I.J. Sobey, The vortex wave membrane bioreactor: hydrodynamics and mass transfer, Chem. Eng. J. 62 (1996) 175–181.

[16] P. Venkateswarlu, N. Jaya Raj, D. Subba Rao, T. Subbaiah, Mass transfer conditions on a perforated electrode support vibrating in an electrolytic cell, Chem. Eng. Process. 41 (2002) 349–356.

[17] N.G. Carpenter, E.P.L. Roberts, Mass transport and residence time characteristics of an oscillatory flow electrochemical reactor, Trans. I. Chem. E 77 (A) (1999) 212–217.

[18] P. Cognet, J. Berlan, G. Lacoste, P. Fabre, M. Jud, Application of metallic foams in an electrochemical pulsed flow reactor: mass transfer performance, J. Appl. Electrochem. 25 (1995) 1105–1112.

[19] G.H. Sedahmmed, M.Z. El-Abd, A.A. Zatout, Y.A. El-Taweel, M.M. Zaki, Mass transfer behavior of electrochemical reactors employing vibrating screen electrodes, J. Electrochem. Soc. 141 (1994) 437–440.

[20] U. Landau, Electro-chemical deposition system and method of electroplating on substrates, US Patent 6,2621,433, July 2001.

[21] R. Omasa, Plating method, US Patent 6,2621,435, July 2001.

[22] A.M. Al Taweel, M.I. Ismail, Comparative analysis of mass transfer at vibrating electrodes, J. Appl. Electrochem. 6 (1976) 559–564.

[23] A.M. Al Taweel, J. Landau, Effect of oscillatory motion on mass transfer between a solid sphere and fluids, Can. J. Chem. Eng. 54 (1976) 532–540.

[24] C.K. Drummond, F.A. Lyman, Mass transfer from a sphere in an oscillating flow with zero mean velocity, Comput. Mech. 6 (1990) 315–326.

[25] M.E. Ralph, Oscillatory flow in wavy-walled tubes, J. Fluid Mech. 168 (1986) 515.

[26] M. Mackley, Use of oscillatory flow to improve performance, Chem. Eng. (London), 433 (1987) 18–20.

[27] V.G. Rodgers, R.E. Sparks, Reduction of membrane fouling in the ultrafiltration of binary protein mixtures, AIChE J. 37 (1991) 39–55.

[28] K. Abel, Influence of oscillatory flows on protein ultrafiltration, J. Mem. Sci. 133 (1997) 39–55.

[29] T. Nishimura, N. Oka, Y. Yoshinak, K. Kunitsugu, Influence of imposed oscillatory frequency on mass transfer enhancement of grooved channels for pulsatile flow, J. Heat Mass Transfer 43 (2000) 2365–2374.
[30] M.A. Leveque, Les lois de la transmission de chaleur par convection, Ann. Mines 13 (1928) 201–299.
[31] F.J. Poulin, G.R. Flierl, J. Pedlosky, Parametric instability in oscillatory shear flows, J. Fluid Mech. 481 (2003) 329–355.
[32] F. Ding, A. Jeffrey Giacomin, R. Byron Bird, C.B. Kweon, Viscous dissipation with fluid inertia in oscillatory shear flow, J. Non-Newton Fluid Mech. 86 (3) (2000) 359–376.
[33] M.Y. Gundogdu, M.O. Carpinlioglu, Oscillatory flow: present state of art on pulsatile flow theory. Part 1. Laminar and transitional flow regimes, JSME Int. J. Ser. B Fluids Therm. Eng. 42 (3) (1999) 384–395.
[34] G.A. Chechkin, A. Friedman, A.L. Piatnitski, The boundary-value problem in domains with very rapidly oscillating boundary, J. Math. Anal. Appl. 231 (1) (1999) 213–235.
[35] D.M. Wang, J.M. Tarbell, An approximate solution for the dynamic response of wall transfer probes, Int. J. Heat Mass Transfer 18 (1993) 4341–4349.
[36] C. Deslouis, O. Gil, B. Tribollet, Frequency response of electrochemical sensors to hydrodynamic fluctuations, J. Fluid Mech. 25 (1990) 85–100.
[37] L. Talbot, J.L. Steinert, The frequency response of electrochemical wall shear probes in pulsatile flow, Trans. ASME 109 (1987) 60–64.
[38] T.J. Pedley, On the forced heat transfer from a hot film embedded in the wall in a two dimensional unsteady flow, J. Fluid Mech. 55 (1972) 329–357.
[39] G. Fortuna, T.J. Hanratty, Frequency response of the boundary layer on wall transfer probes, Int. J. Heat Mass Transfer 14 (1971) 499–1507.
[40] T.J. Pedley, Heat transfer from a hot film in reversing shear flow, J. Fluid Mech. 78 (3) (1976) 513–534.
[41] C.B. Watkins, I.H. Herron, Laminar shear layer due to a thin flat plate oscillating with zero mean velocity, Trans. ASME J. Fluid Eng. 100 (1976) 367–373.
[42] P. Kaiping, Unsteady forced connective heat transfer from a hot film in non-reversing and reversing shear flow, Int. J. Heat Mass Transfer 26 (1983) 545–557.
[43] A.A. Van Steenhoven, F.J.H.M. Van Beucken, Dynamical analysis of wall shear rate measurements, J. Fluid Mech. 231 (1991) 599–614.
[44] Z. Mao, J. Hanratty, Analysis of wall shear probes in large amplitude unsteady flows, Int. J. Heat Mass Transfer 34 (1) (1991) 281–290.
[45] Z. Mao, J. Hanratty, Influence of large amplitude oscillations on turbulent drag, AIChE J. 40 (10) (1994) 1601–1610.
[46] M.B. Liu, E.M. Rudnick, G.M. Cook, N.P. Yao, Mass transfer at longitudinally vibrating vertical electrodes, J. Electrochem. Soc. 129 (1982) 1955–1959.
[47] C.V. Rama Raju, A. Ramalinga Sastry, G.J.V.J. Raju, Ionic mass transfer at vibrating plates, Ind. J. Technol. 7 (1969) 35–38.
[48] R. Lemlich, M.R. Levy, The effect of vibration on natural convective mass transfer, AIChE J. 7 (2) (1961) 240–242.
[49] W.K. Chan, S.L. Lee, C.Y. Liu, Effects of frequency and amplitude of oscillation on low Reynolds number pulsating flow in a circular pipe, Eng. Comput. 19 (1–2) (2002) 119–136.
[50] D.W. Wundrow, M.E. Goldstein, Effect on a laminar boundary layer of small-amplitude streamwise vorticity in the upstream flow, J. Fluid Mech. 426 (2001) 229–263.
[51] S. Eshghy, V.S. Arpaci, J.A. Clark, The effect of longitudinal oscillations on free convection from vertical surfaces, J. Appl. Mech. 39 (1965) 183–191.
[52] F.M. Mahfouz, H.M. Badr, Mixed convection from a cylinder oscillating vertically in a quiescent fluid, Heat Mass Transfer 38 (6) (2002) 477–487.
[53] N. Riley, E.H. Trinh, Steady streaming in an oscillatory inviscid flow, Phys. Fluids 13 (7) (2001) 1956–1961.
[54] E.D. Barbashov, B.F. Glikman, A.A. Kazakov, Experimental study of friction stress on the wall of a cylindrical tube in an oscillating turbulent flow of a liquid, J. Eng. Phys. Thermophys. 73 (4) (2000) 499–692.
[55] H. Schlichiting, Boundary-Layer Theory, seventh ed., McGraw Hill Book Company, New York, 1979, p. 93.
[56] S.W. Churchill, A comprehensive correlating equation for the laminar assisting forced and free convection, AIChE J. 23 (1) (1977) 10–16.
[57] A. Acrivos, Combined laminar free- and forced-convection heat transfer in external flows, AIChE J. 4 (1958) 285–289.